ICANS-XI International Collaboration on Advanced Neutron Sources
KEK, Tsukuba, October 22-26, 1990

Status of the New GLAD Instrument at IPNS*

R. K. Crawford, J. M. Carpenter, R. Dejus, J. R. Haumann, R. Kleb,
D. G. Montague,§ D. L. Price, and S. Susman
Argonne National Laboratory, Argonne, IL 60439.
§On leave from Willamette University, Salem, OR.

ABSTRACT

The complete flight path for the new glass, liquids, and amorphous materials diffractometer (GLAD) at IPNS is now in place, and 160 linear-position-sensitive detectors have been installed. This paper discusses the final instrument configuration and calibration of the instrument. Some of the development of instrument components and data analysis software utilizing the GLAD prototype, which operated for ~ 2 years prior to the installation of GLAD, are also discussed.

I. INTRODUCTION

The new Glass, Liquids, and Amorphous Materials Diffractometer (GLAD), which was been described in detail at an earlier ICANS meeting,[1] has recently been installed at IPNS. In order to develop various components and techniques for the instrument, a prototype flight path with 55 linear-position-sensitive detectors (LPSDs) was operated on the GLAD beamline during 1988-1989. This report summarizes the experience obtained with the prototype flight path for that instrument, the current status of the final version of the instrument, and the status of the data analysis software.

II. INSTRUMENT STATUS

The main vacuum tank arrived at IPNS in December, 1989. The prototype flight path was removed and the final flight path, evacuated scattering chamber, detectors, and shielding were installed during Spring, 1990. The first measurements with a sample in the new flight path were made in July, 1990. Figure 1 shows what GLAD looks like in relation to the adjacent instruments,

*Work supported by U.S. Department of Energy, BES, contract No. W-31-109-ENG-38.

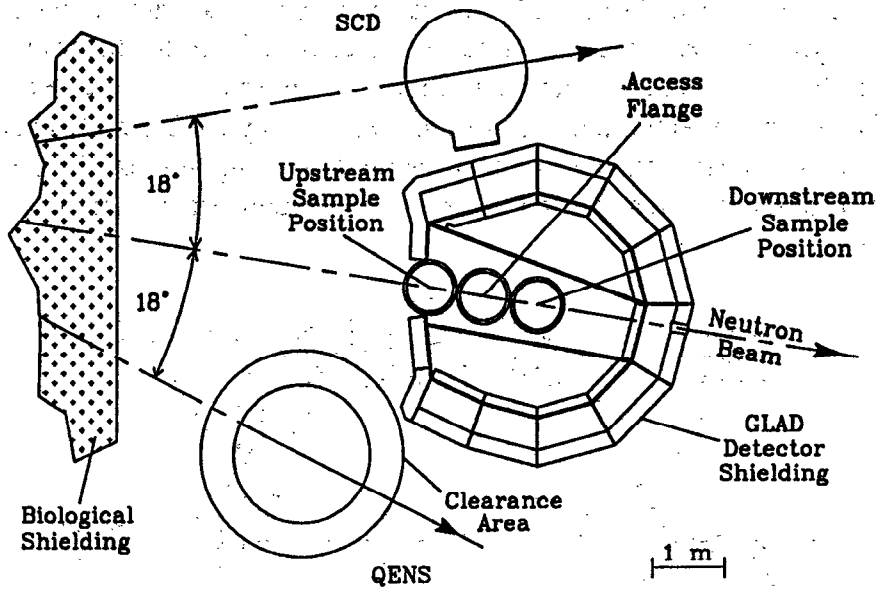

Figure 1. Schematic of the final layout for GLAD in relation to the adjacent instruments SCD and QENS.

QENS and SCD. GLAD has two sample positions, an upstream position 9.0 m from the moderator for the highest resolution measurements and a downstream position 10.5 m from the moderator, which provides higher data rates at some sacrifice in resolution. Crossed converging soller collimators focused on the forward detector bank provide the final collimation for the thermal and epithermal neutrons used by GLAD. With this collimation scheme the sample size does not contribute significantly to the resolution,[2] so samples up to ~2.5 x 2.5 cm^2 can be used at the upstream position. A series of massive apertures upstream from the soller collimators serves to define the beam, and is the primary collimation for those higher-energy neutrons for which the soller collimators become transparent. The last of these massive apertures can be adjusted to control the beam size to minimize the amount of background when smaller sample sizes are used. The flight path is evacuated and the detectors are located outside this vacuum, viewing the sample positions through thin Al windows.

The evacuated flight path, soller collimators, and detector modules are shown in Fig. 2, which also indicates the locations of the detectors near the inner edges of the modules. When the upstream sample position is used this detector locus is approximately the focusing locus for the soller collimators,[2] although some compromises have been made at the higher scattering angles in order to optimize the total resolution. All of the GLAD detectors are LPSDs, and there are 160 LPSDs mounted in 4 detector modules in the final version of GLAD at this stage. Each of these LPSDs is a cylindrical gas-proportional-counter, 1.11 cm inside dia x 60 cm active volume, filled with 10 atm of ^3He, and encoded into 64 segments by charge-division encoding. These 160 LPSDs completely fill three detector modules at low angles and partially fill a fourth module at the higher angles. These modules are indicated in Fig. 2. In order to cover as small scattering angles as possible, the LPSDs in the forward detector module extend through the path of the direct beam. A small B_4C "beam attenuator", described in detail elsewhere,[3] is located in the beam upstream from these LPSDs (see Fig. 2) to absorb enough of the direct beam to protect these LPSDs from

significant overload. The currently-installed detectors cover scattering angles from -9° to +47° for the upstream sample position and from -17° to +95° for the downstream sample position, with the negative sign implying scattering angles measured clockwise from the direct beam when viewed from above, as in Fig. 2. Angular coverage is continuous over these ranges except for the small gaps between the detector modules and the portions excluded by the beam attenuator at very-small scattering angles. The beam attenuator obscures the scattering angles $|2\theta| < 1.7°$ when the upstream sample position is used and $|2\theta| < 3.4°$ when the downstream sample position is used.

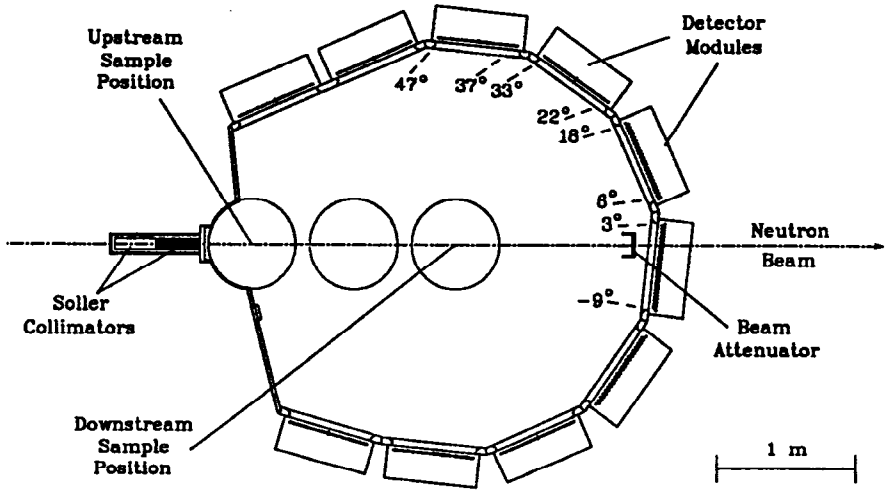

Figure 2. GLAD evacuated scattering chamber and detector modules. The limiting scattering angles, relative to the upstream sample position, are shown for the four detector modules now installed. The remaining six planned detector banks are also shown in their correct locations, but with no angle indications. The actual detector modules holding the banks of LPSDs are similar to the one shown in Fig. 3. The soller collimators and the beam attenuator which protects the LPSDs at small angles from the direct beam are also shown.

For incident neutrons having a wavelength of 0.1 Å, the currently-installed LPSDs will produce a maximum Q of 50.5 $Å^{-1}$ and 92.6 $Å^{-1}$ for the upstream and downstream sample positions respectively, although the quality of the data over this full Q range remains to be seen. Within the next 3-4 years the remainder of the 10 detector modules will be filled, raising the total to 408 LPSDs and providing angular coverage from -76° to +95° for the upstream sample position and -134° to +150° for the downstream position. As shown in the figure, the locations of the detector modules on the two sides of the flight path are not symmetric, so that when the full complement of detectors is installed the scattering angles not covered on one side of the flight path will be covered on the other.

Prior to the installation of GLAD, the IPNS powder diffractometers SEPD and GPPD were used for diffraction studies of amorphous materials. The intensity of the incident neutron beam for GLAD is approximately twice that at SEPD and four times that at GPPD. Furthermore, GLAD detectors will eventually cover several times the solid angle spanned by those on SEPD or GPPD, so the demands on the TOF data acquisition system are much more severe for GLAD than on the previous instruments. The new FASTDAS system[4] has been developed to respond to these higher instantaneous and time-averaged counting rates on GLAD.

As part of the correction procedures for analyzing diffraction data for glasses and liquids it is important to measure the sample attenuation characteristics. Considerable effort was expended to develop a transmission monitor[3] for this purpose as well as to improve the accuracy and response of the incident beam monitor.[5] Results of such transmission measurements are described elsewhere in these proceedings.[3]

III. TESTS USING THE PROTOTYPE FLIGHT PATH

Configuration

The final tests with the prototype flight path were completed in December 1989. Measurements were made on various samples and calibrants, including vanadium, SiO_2, polyethylene, diamond powder, intercalates and zeolites, iridium and hafnium, germanium, nickel, and beryllium. Figure 3 shows schematically the prototype flight path arrangement including the variable aperture, beam monitor, soller collimators, sample chamber, B_4C beam attenuator, and the

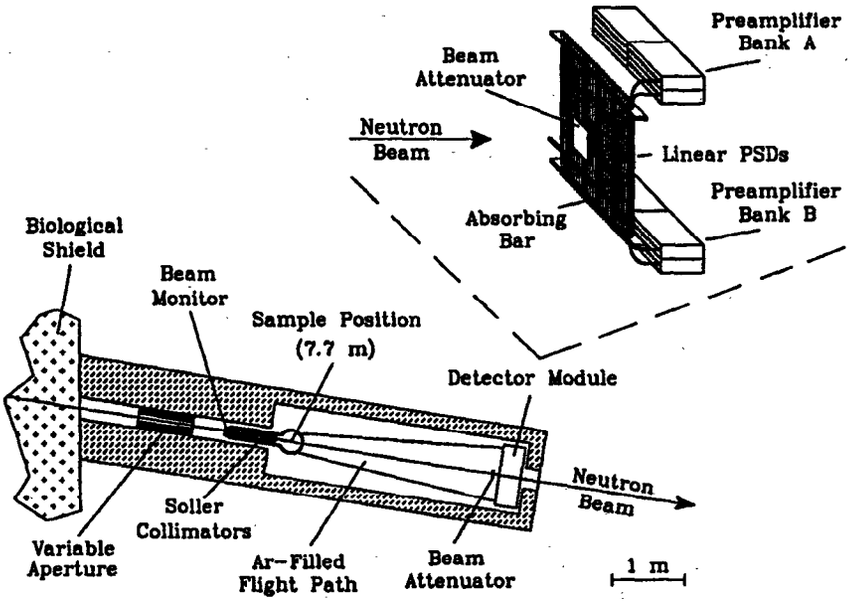

Figure 3. The prototype GLAD flight path in use during 1988-1989. The inset to the figure shows details of the detector module along with the relative locations of the beam attenuator and the absorbing bar used in calibrating the LPSDs. Each detector module in the final version of GLAD is identical to this except for some details of the positioning of the LPSDs within the individual modules.

single detector module. The path between the sample chamber and the detectors on this prototype instrument was not evacuated. Instead it was filled with a low pressure flow of Ar gas to force out the air and water vapor which would otherwise be in the scattered neutron flight path and would produce a large background due to scattering from the main beam. The sample position was at 7.7 m from the moderator and the detector module was centered on the direct beam at 10.7 m from the moderator. This module was protected from the direct beam by a beam attenuator, and contained a complement of 55 LPSDs of the same type as are now in the final instrument. Each of these

LPSDs had charge sensitive preamplifiers top and bottom, and the positions of the detected neutrons were determined by the charge-division method. The detectors were placed for complete area coverage in such a way that the active area of each tube was not shadowed by an adjacent detector. The position encoding resolution was about 1.4 cm, so the data were binned in 2-segment groupings for a total of 1540 individual detection areas of ~1 cm x 2 cm. Angular coverage in scattering measurements ranged from a lower limit of about 2°, limited by background near the penumbra of the beam of high energy neutrons, to a maximum of ~8° at the tops and bottoms of the end detectors. The range of time-of-flight (TOF) values used for most measurements was 200 μs to 12,000 μs, which corresponds to a wavelength range from 0.07 Å to 4.4 Å.

Calibration

The prototype flight path was very useful for developing techniques for both angle and wavelength calibration of GLAD. For angle calibration the most useful samples have been diamond powder and several different intercalation compounds. Additional angular calibration is available from the measured instrument geometry and from the flood-pattern measurements with an absorbing bar at various positions in front of the LPSDs. Figure 4 shows the results for diffraction from a powder sample of stage-2 cesium-intercalated graphite. The figure includes data from all of the segments as a function of TOF for one of the LPSDs at the end of the detector array. Each trace

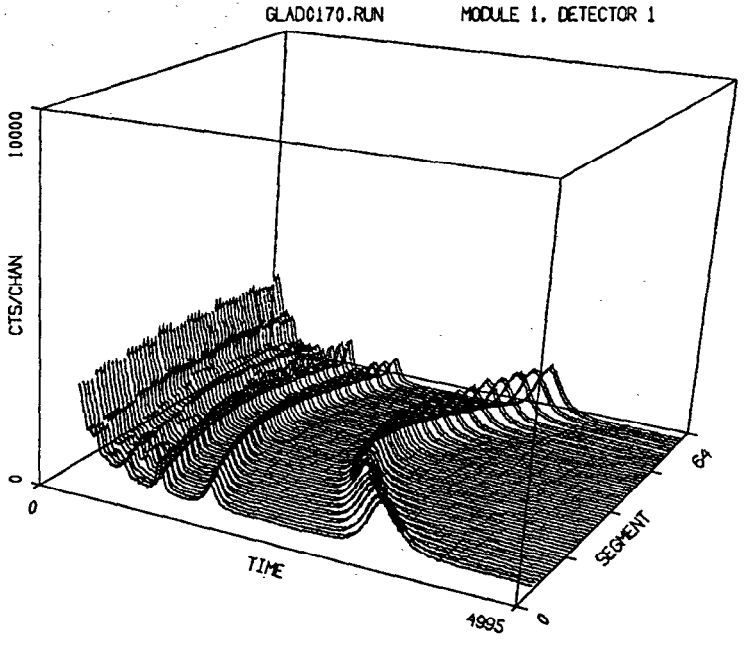

Figure 4. Bragg peaks from a powder sample of stage-2 cesium-intercalated graphite illustrating the "diffraction rings" for the LPSD centered at 6.1°. The maximum scattering angle is 8.0° for the end segments of this detector.

in the figure gives the detector response for a single segment of ~1 cm length from a single LPSD. However since pairs of such segments were grouped together during the histograming process, each independent TOF histogram corresponds to a ~2 cm length of the LPSD and appears as a double trace in the figure. The central segments in this figure correspond to a scattering angle of ~6.1°

and the end segments correspond to scattering angles of ~8.0°. At least four Bragg peaks are clearly observed for each segment, and for the end segments these occur at 754 μs, 1163 μs, 1726 μs, and 3515 μs. The peak at 3515 μs corresponds to Bragg scattering which occurs at a d-spacing of 9.33 Å for this sample, indicating that the average scattering angle for the end segments of this LPSD is 7.97°. The angle-TOF correlation of the Bragg peak positions is clearly evident as "diffraction rings" in the data displayed in this manner.

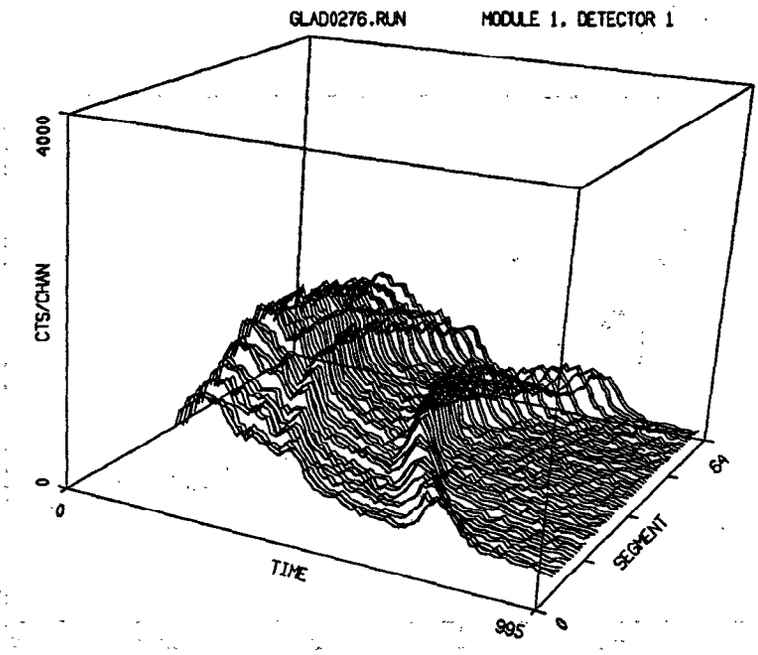

Figure 5. The use of diamond powder as a scatterer for angle calibration purposes.

Figure 5 illustrates the scattering measured for diamond into one of the end LPSDs for TOFs from 200 μs to 1000 μs. The peak positions yield the angle calibration and the widths the resolution. Most of the peak widths indicated in the figure reflect the range of scattering angles sampled by these two paired LPSD segments, rather than any intrinsic timing resolution. Note that the TOF range is about one-sixth of that in Fig. 4 and the "diffraction rings" are still very clear. We obtain a single segment resolution ($\Delta Q/Q$) at $Q = 0.5$ Å^{-1} of about 0.075 at the center of the detector and 0.10 near the top of the detector. The differences here are primarily due to the geometrical effects of the rectangular segment shape. The resolution is nearly twice as broad at the top and bottom of the central LPSDs of the array as compared to the center of the end LPSD because of this geometrical effect.

On SEPD and GPPD, angular data are time-focused into eight separate detector groups before the data are histogramed and stored into a run file, so for these instruments final wavelength and angle calibration is done for these eight focused detector banks rather than for the individual detectors. On GLAD, angular data are not time-focused into groups before the data are stored in a run file, although separate detector segments at the same scattering angle may be grouped together on-the-fly. Thus on GLAD it is necessary to calibrate every segment for wavelength-vs-TOF as well as for angle. We have had to rely on nuclear absorption resonances and Bragg scattering from crystalline materials to determine the wavelength of the incident neutrons as recorded by TOF in the individual segments. Figure 6 shows the TOF spectrum obtained in one of the LPSD segments

when an iridium foil was placed in the incident beam and an "isotropic" scatterer (polyethylene) was placed at the sample position. The three lowest energy resonances of iridium are at energies of 0.656, 1.303, and 5.36 eV (wavelengths of 0.353, 0.251, and 0.124 Å respectively), and these are clearly observed in the figure as depressions at approximately 960, 680, and 330 μs respectively. Measurements have also been made using hafnium foils, oriented nickel and germanium single crystals, and nickel and beryllium polycrystals as incident beam filters to provide a range of wavelength calibrations up to 4 Å.

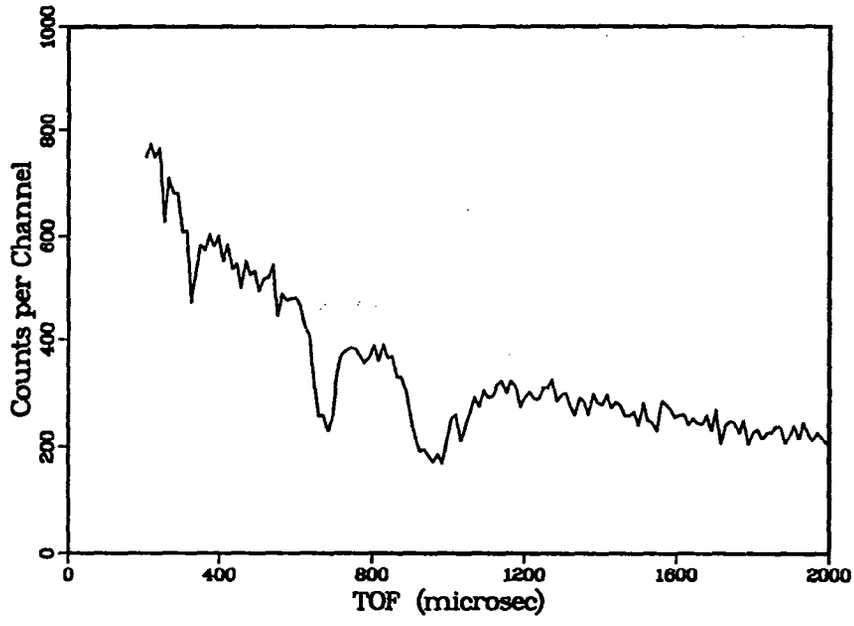

Figure 6. The use of iridium as an absorber for wavelength calibration purposes.

Scattering Data

Results measured on this prototype flight path for the S(Q) for a 0.37 cm plate and a 0.9 cm rod of SiO_2 are shown in Fig. 7, where they are compared with similar data from SEPD. Data reductions for the GLAD temporary flight path data utilized the GLAD analysis software discussed below. The measurements with the prototype GLAD flight path extend the Q-range down to near 0.1 $Å^{-1}$, while the upper limit of Q is 4.2 $Å^{-1}$ for 0.2 Å incident neutrons. Measurements were also made with the SiO_2 rod in the vanadium foil ("Howe") furnace and in an 8 kbar aluminum pressure cell as a test of the data analysis programs. Measurements on a smaller SiO_2 rod (0.4 cm) were also performed. Although they were limited by the scattering from the argon gas, these results indicated that the sensitivity of the small-angle detector array was good.

IV. ANCILLARY EQUIPMENT

Provision has been made on the final GLAD instrument for rapid evacuation of the total scattering chamber. Apparatus has been designed and assembled to provide automated control of sample environments. A 10-position, room-temperature sample changer has been constructed and

tested, and a 5-position, low temperature (10 K to 300 K) sample changer is in the final stages of assembly and calibration. High pressure capability is provided by a hydraulic system fitted with an 8 kbar aluminum cell or with an 8 kbar Rene-41 cell intended for work at elevated temperatures. The pressure system has been tested and is being calibrated. As mentioned above, a high-temperature (300 K to 1300 K) vanadium foil furnace has been tested in the prototype flight path. Preliminary indications are that experimental data obtained using this furnace are contaminated by secondary scattering from the furnace mounts, so this problem is under study.

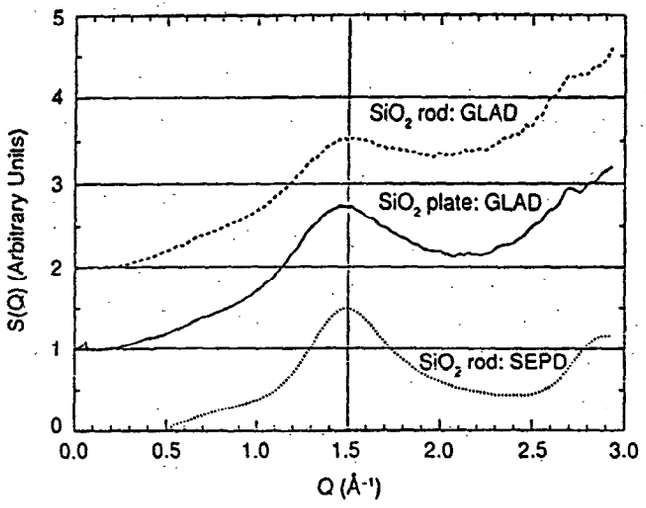

Figure 7. Comparison of SiO_2 scattering results measured on SEPD and on GLAD.

V. ANALYSIS SOFTWARE

A large effort has been devoted to the development of efficient and structured computer programs for the analysis of scattering from amorphous and liquid materials at IPNS. The programs have been developed on the VAX series of computers using VAX FORTRAN (Digital Equipment Corporation, Maynard, MA, USA), commercial NAG-library routines (Numerical Algorithms Group Ltd, Oxford, UK), and other library routines developed locally at Argonne. Plotting routines utilize either CA-DISSPLA Version 11.0 (Computer Associates International, Inc., Garden City, NY, USA) or the IPNS GPLOT GKS-based graphics routines.[6]

An experiment on GLAD is started by first setting up a run file which contains information about how LPSD segments are grouped together and how the TOF histograms are organized. There are virtually no restrictions on how this may be achieved; for example, detector segments may be grouped into Debye-Scherrer cones (preferable for isotropic scattering) and the time fields may be chosen with a channel width which is proportional to the TOF. In addition the run file contains calibration information concerning scattering angles, distances, etc. which are needed in the subsequent data analysis. The run files are large (up to ~12 Mbyte = 24,000 blocks on the VAX), and even though the packing density of data on mass storage devices is increasing steadily, the amount of data generated by GLAD will be enormous by any standard. A typical experiment will encompass several run files generated in a short period of time, which will be the case, in particular,

when one of the automatic sample changers is used. Hence, efficient programs must be available for analyzing the data and compressing it to more manageable sizes. The raw run files will be archived on secondary mass storage devices (currently 8-mm tapes holding about 2 Gbytes each) after the first-step analysis.

The analysis may be divided into several distinct tasks. The first step is carried out by the INTENSITY program. This program reads the "raw" data from the binary run files and examines the detector grouping and the TOF histograming at the time of data collection. The program then re-groups the data as the user chooses (e.g. redundant information may be grouped together after checking for spurious behavior) and normalizes the scattering to the incident beam spectrum and subtracts background scattering. The conversion from TOF to wavelength is also made in this program. The converted data are stored in a file as a function of scattering angle and wavelength.

The next step is to calculate the correction coefficients which are applied to the data subsequently by the STRUCTURE FACTOR program. The CORRECTIONS program calculates the absorption corrections for the reference scatterer (typically vanadium), the sample, and the container by the method of Paalman and Pings,[7] and calculates the multiple scattering by the method of Blech and Averbach.[8] At present, the corrections assume either a cylindrical sample geometry or a flat plate sample geometry. However, corrections for other geometries are under development, some of them based on routines developed at ISIS[9] in the UK. Experiments utilizing special environments place high demands on reliable correction routines, and much future work will be devoted to this subject.

The STRUCTURE FACTOR program applies the corrections to the data and normalizes to the reference run. The inelasticity (Placzek) corrections[10] are also calculated and applied in this program. Each detector group is still treated separately, and the output contains the structure factor for every group (each at a slightly different angle) as a function of the scattering vector Q which has been calculated from the wavelength and the scattering angle.

The TRANSFORM program typically combines the data (flux or counting-statistics weighting) from the different detector groups into a "single" structure factor S(Q) which will cover a range from approximately 0.1 - 40 $Å^{-1}$ or higher when the full complement of detectors at high angles is installed in GLAD. Then, the structure factor is transformed into real-space via the Fast Fourier Transform technique. Various real-space correlation functions may be calculated which then can be analyzed in terms of bond-lengths, coordination numbers, vibrational amplitudes, etc. A program for fitting overlapping peaks, which accounts for the broadening introduced by the finite upper integration limit, also is available.

Acknowledgments

The efforts of the following in the design and construction of GLAD are gratefully acknowledged: D. Bohringer, T. Bush, M. Faber, J. Jorgensen, D. Leach, G. Ostrowski, J. Richardson, A. Schulke, and K. Volin. The efforts of the following students from Willamette University are also acknowledged: D. Bloom, R. Colleran, D. Gipp, B. Haagensen, and L. Moen.

References

1. R. K. Crawford, D. L. Price, J. R. Haumann, R. Kleb, D. G. Montague, J. M. Carpenter, S. Susman, and R. J. Dejus. Advanced Neutron Sources 1988, Proceedings of the 10th Meeting of the International Collaboration on Advanced Neutron Sources (ICANS X), held at the Los Alamos National Laboratory, Oct. 3-7, 1988. Institute of Physics Conference Series Number 97, IOP Publishing Ltd, New York. pp 419-426 (1989).
2. A. C. Nunes. Nucl. Instr. and Meth. 119, 291-293 (1974).
3. D. G. Montague, J. M. Carpenter, R. K. Crawford, R. Dejus, D. L. Price, and S. Susman. "Use of a Semi-Opaque Beamstop for Monitoring Sample Transmissions at GLAD", these proceedings.
4. R. K. Crawford and J. R. Haumann. IEEE Trans. Nucl. Sci. NS-37, 72-81 (1990).
5. R. K. Crawford, J. R. Haumann, and G. E. Ostrowski. "Neutron Detectors at IPNS", these proceedings.
6. T. G. Worlton. Proc. DECUS Spring Symp., 105-117 (1988).
7. H. H. Paalman and C. J. Pings, J. Appl. Phys. 33(8), 2635-2639, (1962).
8. I. A. Blech and B. L. Averbach, Phys. Rev. 137(4A), A1113-A1116, (1965).
9. A. K. Soper, W. S. Howells, and A. C. Hannon, Rutherford Appleton Laboratory, RAL-89-046, (1989).
10. M. Misawa, D. L. Price, and K. Suzuki, J. Non-Cryst. Solids, 37, 85-97, (1980).